KTH Industrial Engineering
and Management

Adhesion in the wheel–rail contact under contaminated conditions

Yi Zhu

Licentiate thesis
Department of Machine Design
Royal Institute of Technology
SE-100 44 Stockholm

TRITA – MMK 2011:15
ISSN 1400-1179
ISRN/KTH/MMK/R-11/15-SE
ISBN 978-91-7501-181-3

TRITA – MMK 2011:15
ISSN 1400-1179
ISRN/KTH/MMK/R-11/15-SE
ISBN 978-91-7501-181-3

Adhesion in the wheel–rail contact under contaminated conditions

Yi Zhu, yiz@kth.se

Licentiate thesis

Academic thesis, which with the approval of Kungliga Tekniska Högskolan, will be presented for public review in fulfillment of the requirements for a Licentiate of Engineering in Machine Design. Public review: Kungliga Tekniska Högskolan, Room B 242, Brivellvägen 85, Stockholm, on December 1, 2011, at 10:00

Printed in Sweden

Universitetsservice US-AB

Abstract

Railway vehicles require a certain level of adhesion between wheel and rail to operate efficiently, reliably, and economically. Different levels of adhesion are needed depending on the vehicle running conditions. In the wheel tread–railhead contact, the dominant problem is low adhesion, as low adhesion on the railhead negatively affects railway operation: on one hand, the vehicle will lose traction resulting in delay when driving on low-adhesion tracks; on the other hand, low adhesion during deceleration will extend the braking distance, which is a safety issue.

This thesis examines the influence of several contaminants, i.e., water, oil, and leaves, on the adhesion in the wheel tread–railhead contact. This study will improve our knowledge of the low-adhesion mechanism and of how various contaminants influence adhesion. The thesis consists of a summary overview of the topic and three appended papers (**A**–**C**).

Papers **A** and **B** focus mainly on water and oil contamination examined using two methods, numerical simulation and lab testing. In paper **A**, real measured wheel and rail surfaces, low- and high-roughness surfaces, along with generated smooth surfaces are used as input to the numerical model for predicting the adhesion coefficient. Water-lubricated, oil-lubricated, and dry contacts are simulated in the model. In the research reported in paper **B**, scaled testing using a mini traction machine (MTM) was carried out to simulate the wheel–rail contact under lubricated conditions. Two types of disc surfaces of different roughnesses were run at different contact pressures and temperatures. A stylus machine and atomic force microscopy (AFM) were used to measure the surface topography. A study of leaf contamination on the railhead surface, based on field testing, is presented in paper **C**. Railhead surface samples were cut and the friction coefficient was measured on five occasions over the course of a year. Electron spectroscopy for chemical analysis (ESCA) and glow discharge optical emission spectrometry (GD-OES) were used to detect the chemical composition of the leaf-contamination layer on the railhead surface.

The main conclusion of the thesis is that different contaminants reduce the adhesion coefficient in different ways. Oil reduces the adhesion coefficient by carrying the normal force due to its high viscosity. Water can reduce the adhesion coefficient to different degrees depending on the surface topography and water temperature. The mixture of an oxide layer and water contamination may have an essential impact. A leaf-formed blackish layer causes low adhesion by means of a chemical reaction between the leaves and bulk material. The thickness of the friction-reducing oxide layer predicts the friction coefficient and the extent of leaf contamination.

Keywords: Adhesion; Wheel–rail contact; Contaminants; Rough surfaces.

Preface

The work in this thesis was carried out between September 2009 and October 2011 at the Department of Machine Design at Royal Institute of Technology (KTH), Stockholm, Sweden.

I would like to thank the SAMBA Swedish research programme and especially Trafikverket, SL and Railway Group at KTH for funding this project. My main supervisor Ulf Olofsson deserves particular thanks for giving me the chance to do this work, guiding me into the field of tribology and for his excellent guidances and encouragements. Special thanks also to Anders Söderberg as my co-supervisor for discussions and many good comments, Stefan Björklund for the discussion of contact mechanics, Saeed Abbassi for teaching me lots of railway technology, Ellen Bergseth for teaching me to use stylus machine and AFM, Peter Carlsson for helping me during the field test, Karin Persson and Rickard Nilsson as my papers' co-authors, Johan Andersson for your help during MTM testing, and all of my colleagues.

In addition, I want to gratefully acknowledge all my friends for being with me chatting and playing together.

Finally, I want to show my most heartfelt gratitude to my family, especially my dad and mum, for your supports and encouragements during my overseas study. Your efforts are beyond any words to be expressed!

Stockholm, October 2011

Yi Zhu

List of appended papers

This thesis consists of a summary and the following appended papers:

Paper A

Y. Zhu, U. Olofsson, A. Söderberg: "Adhesion modeling in the wheel–rail contact under dry and lubricated conditions using measured 3D surfaces".

This paper was submitted to *Journal of tribology*. This paper is an extended version of : Y. Zhu, U. Olofsson, A. Söderberg , "Adhesion modeling in the wheel–rail contact under wet conditions using measured 3D surfaces", *Proceedings of IAVSD 2011: International Symposium on Dynamic of Vehicles on road and tracks,* Aug 14-19, 2011, Manchester, UK.

The main part of the writing and adhesion modelling were performed by Zhu.

Paper B

Y. Zhu, U. Olofsson, K. Persson: "Investigation of factors influencing wheel–rail adhesion using a mini traction machine".

This paper was submitted to *Wear*.

The experimental works and the main part of the writing were performed by Zhu.

Paper C

Y. Zhu, U. Olofsson, R. Nilsson: "A field test study of leaf contamination on the rail head surfaces".

This paper was submitted to *The first International conference on Railway Technology: Research, Development and Maintenance,* Apr 18-20, 2012, Las Palmas de Gran Canaria, Spain

The main part of the writing and evaluation were performed by Zhu.

List of published papers not included in this thesis

R. Lewis, S. Lewis, Y. Zhu, S. Abbasi, U. Olofsson: "The modification of a slip resistance meter for measurement of railhead adhesion", *IHHA 2011: International Heavy Haul Association Conference*, Jun 19-22, 2011, Calgary, Canada.

Contents

Appended papers

A. Adhesion modelling in the wheel–rail contact under dry and lubricated conditions using measured 3D surfaces
B. Investigation of factors influencing wheel–rail adhesion using a mini traction machine
C. A field test study of leaf contamination on railhead surfaces

1 Introduction

Railway vehicle operation depends on the adhesion between the wheel and rail. To run such vehicles efficiently and economically, the wheel–rail adhesion should be maintained at a certain level. According to the vehicle running conditions, wheel–rail contact is generally divided into two types, wheel tread–railhead contact on straight track and wheel flange–rail gauge contact on curved track. In most cases, flange contact requires a low adhesion coefficient to reduce wear and noise, while tread contact requires a comparatively high adhesion coefficient to obtain good accelerating and decelerating ability.

This thesis examines poor adhesion in the wheel tread–railhead contact, since this causes problems [1]. First, it affects vehicle performance because the vehicle will lose traction when driving on low-adhesion track. Moreover, low adhesion is also a safety issue, since poor adhesion when decelerating will extend braking distances. Since the wheel–rail contact is an open system, many environmental factors can contribute to low adhesion on the railhead. Common contaminants resulting in low adhesion are water, oil or grease and a leaf-formed blackish layer.

The overall goal of this thesis is to investigate the influence of contaminants (i.e., water, oil, and leaves) on the adhesion coefficient in the wheel tread–railhead contact, bearing in mind that different contaminants affect the adhesion differently. An enhanced understanding of the mechanism of low adhesion could help in predicting the adhesion coefficient in the wheel–rail contact and in finding a way to alleviate the poor adhesion problem.

The work addresses the following research questions:

- How does surface topography affect wheel–rail adhesion under water-lubricated conditions?
- How does surface topography affect wheel–rail adhesion under oil-lubricated conditions?
- Do other factors affect wheel–rail adhesion?
- What is the chemical composition of the leaf-contaminated blackish layer, and how does it differ from those of uncontaminated layers?
- Why does the presence of a leaf-formed blackish layer on the railhead surface give a low friction coefficient?

The methodology used here is briefly summarized in Fig. 1. This thesis deals with the low adhesion problems caused by contamination with water, oil, and the leaf-formed blackish layer. The influence of water and oil on the adhesion coefficient is studied based on computer simulation with a numerical model (paper **A**) and lab testing using a mini traction machine (paper **B**). In both papers **A** and **B**, the wheel–rail contact is also examined under dry conditions for purposes of comparison. Leaf contamination on the railhead surface is discussed in paper **C** with reference to a field test.

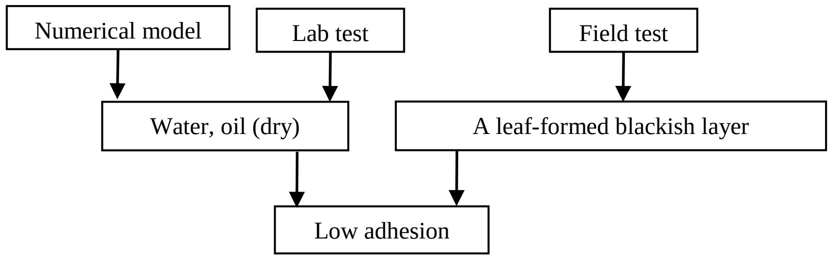

Figure 1. Schematic of the methodology of the thesis.

The thesis is structured as follows:

Chapter 2 presents the fundamentals of the wheel–rail contact. Chapter 3 discusses the fundamentals of various contaminants and their influence on the adhesion coefficient. Chapters 4–6 present the methodology used to investigate low adhesion under contaminated conditions based on numerical modelling, laboratory testing, and field testing. Summaries and the results of papers **A**–**C** are also briefly presented in these chapters. Chapter 7 presents the concluding remarks, which answer the research questions. Papers **A**–**C** are appended at the end of the thesis.

2 Adhesion in the wheel–rail contact

2.1 Wheel–rail contact conditions

Unlike road vehicles, such as the automobile, railway vehicles have some unique behaviours and properties, such as hunting motion, self-steering capability, and lateral dynamics. These unique features originate from the wheel–rail guidance system depending on wheel and rail geometry. First, the rail has a specific profile [2], governed by rules, and is mounted at a small inwards inclination (1:30 in Sweden) (indicated by no. 3 in Fig. 2) for better fit to the wheel profile and better load transfer to the sleepers and ballast. Second, the wheel is of a special design, including a wheel tread (where contact point 1 is located on the wheel in Fig. 2) and wheel flange (where contact point 2 is located on the wheel in Fig. 2). Moreover, the wheel profiles are usually conical (indicated by no. 4 in Fig. 2), leading to the difference in rolling radius in a curve for the two wheels in the same wheelset. Compared with tire–road interaction, the wheel–rail contact is very small at approximately 1 cm^2 [1]. As a result, the heavy axle load is transferred through a small patch generating high contact pressure.

Due to the above-mentioned factors, the wheel–rail contact area changes when running under different conditions. Generally, when the vehicle is running on a straight track, the contact area is usually between the wheel tread and railhead, as shown by contact point 1 in Fig. 2. When the vehicle is running on a curve, the contact area moves to between the wheel flange and rail gauge, as shown by contact point 2 in Fig. 2, or both of contact point 1 and 2. However, in real operation, the wheel rail contact varies constantly in terms of area and type, even starting from the same profile. In railway maintenance, wheels need to be changed and rails need to be re-ground after a certain time, depending on the contact conditions and wear.

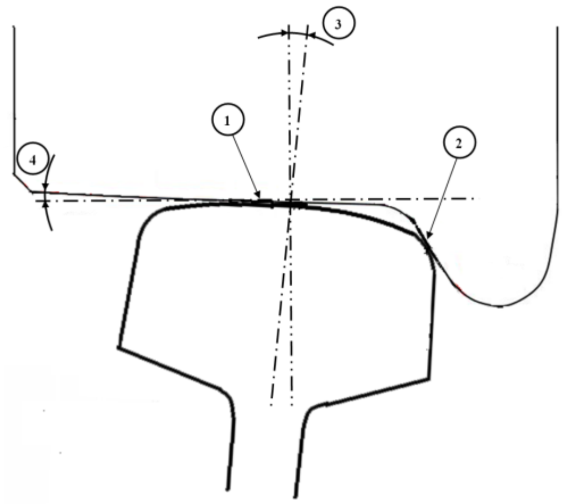

Figure 2. Schematic of two types of wheel–rail contact: 1. wheel tread–railhead contact and 2. wheel flange–rail gauge contact; 3. rail inclination; 4. conical wheel profile.

The two basic types of wheel–rail contact differ in many respects. Lewis and Olofsson [3] presented the operating conditions in a wheel tread–railhead contact and a wheel flange–

rail gauge contact, as shown in Fig. 3. As the contact area changes from wheel tread with railhead to wheel flange with rail gauge, both contact pressure and sliding velocity increase significantly. According to Olofsson and Telliskivi [4], rail hardness also has clear dependence on the contact type. In addition, the wear rate at the rail gauge is 10 times greater than the wear rate at the railhead [3]. In the present work, we will discuss only the wheel tread–railhead contact, which assumes that the vehicle is running on a straight track, and only longitudinal creep is considered. In the following sections, all discussions are based on this assumption.

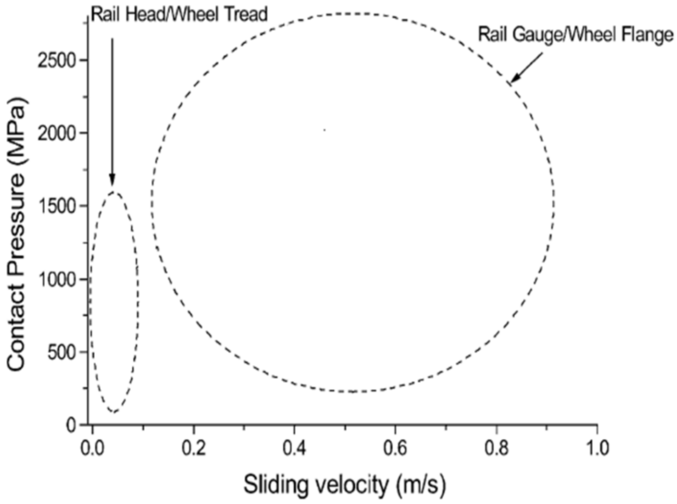

Figure 3. Contact conditions in a wheel rail contact [3].

The wheel–rail contact is a rolling–sliding contact. It is easy to imagine wheels rolling on tracks. On the other hand, wheels will also spin if the tracks are very slippery, for example, if there is ice on the track, in what is known as sliding motion. The combination of the two motions is called rolling–sliding contact. The difference between the circumferential velocity of a driven wheel and the translational velocity of the wheel over the track is usually a non-zero value, which is known as sliding velocity u_s. The ratio of sliding velocity to rolling velocity is called creep or creepage [5], which is the main source of creep force. In this thesis, we relate creep to a positive value assuming the vehicle is braking.

$$\xi = u_s / u_r = (u_v - u_w) / u_r \tag{1}$$

where u_v is the vehicle running speed or translational velocity of a wheel over a rail, u_w is the circumferential velocity of a wheel, and u_r is the rolling speed, defined as follows [5][6]:

$$u_r = (u_v + u_w) / 2 \tag{2}$$

Note that many sources treating railway dynamics define creep as the ratio of sliding velocity to vehicle speed, assuming very small creep. In wheel flange–rail gauge contact, creep is high, resulting in high sliding velocity, while in wheel tread–railhead contact, creep is usually relatively small.

When creep is zero (here we only consider longitudinal creep), which is a pure rolling case, no tangential force is transmitted and the contact area sticks. As soon as tangential force starts to be transmitted, a slip region appears in the trailing edge of the contact patch, while the rest of the contact patch remains stick. This stick–slip region results in rolling–sliding contact. The slip region increases and the stick region decreases in size with increasing creep. When the creep is high enough, the stick region disappears leading to gross slip. The relationship between tangential force and creep is presented in Fig. 4.

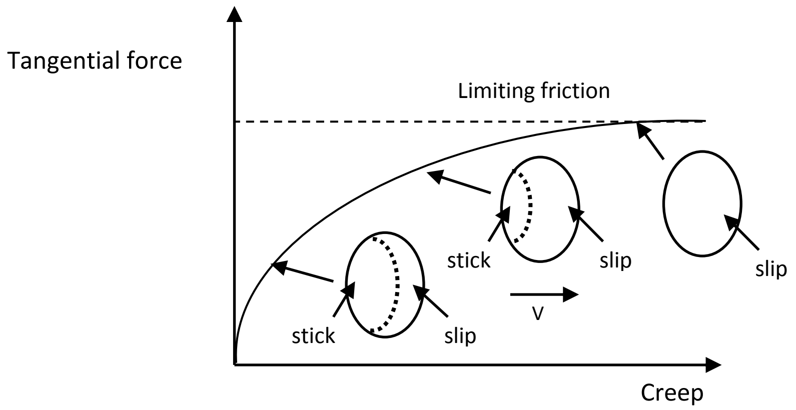

Figure 4. Relationship between tangential force and creep.

2.2 Friction and adhesion

In the late sixteenth century, Leonardo Da Vinci started systematically studying friction. Friction is defined as "the resisting force tangential to the common boundary between two bodies when, under the action of an external force, one body moves or tends to move relative to the surface of the other" [7]. Friction is usually represented by the friction coefficient, which is defined as the ratio of the friction force (F_f) and the normal force (F_N) in the contact between two surfaces, as given in Eq. 3:

$$\mu = \frac{F_f}{F_N} \tag{3}$$

In a railway context, 'adhesion' is the friction available to transmit tangential force between railway wheel and rail [1]. Therefore, the vertical axis in Fig. 4 could also be labelled 'adhesion'. The term 'adhesion' is used by both braking and driving wheels. Note that some studies use the term 'traction coefficient' instead of 'adhesion coefficient', presumably because the research examined traction conditions, i.e., the wheels accelerating over the rail. The adhesion coefficient ($\mu_{adhesion}$) is limited by the friction coefficient ($\mu_{friction}$), which is defined as follows:

$$\mu_{adhesion} = \frac{F_T}{F_N} \leq \mu_{friction} \tag{4}$$

where F_T is the tangential force or adhesion.

The two types of wheel–rail contact require different adhesion levels, which are limited by the friction coefficient. Ideal friction coefficients in the wheel–rail contact [1] for heavy haul traffic are shown in Fig. 5. When the vehicle is running on a straight track, high adhesion is desirable: during acceleration, low adhesion causes performance problems resulting in delays, while during deceleration, low adhesion dangerously extends the braking distance [1]. Adhesion coefficient requirements for braking and traction [8–10] are listed in Table 1. On the other hand, when the vehicle is travelling around curves, high adhesion in, for example, sharp curves, will also generate problems. In the worst case, excessive adhesion in curves causes wheel climb derailment, as in the 8 March 2000 train accident on a Tokyo metro line [11]. Since low adhesion is desirable in the wheel flange–rail gauge contact, lubricant is usually applied to curved rails. Adhesion in the wheel tread–railhead contact is expected to be comparatively high, so lubrication should be avoided. In some cases, a friction modifier is applied to keep the friction coefficient within a desirable range. According to field measurements [4], the coefficient of friction is higher on the railhead than on the rail edge. However, since the rail is open to the environment, many factors can affect railway adhesion, which will be discussed in the next chapter.

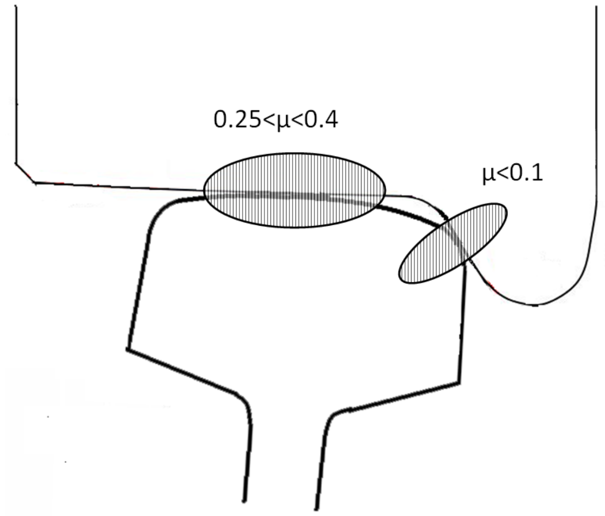

Figure 5. Ideal friction coefficients in the wheel–rail contact for heavy haul traffic [1].

Table 1. Required adhesion coefficients.

	Adhesion coefficient for braking	**Adhesion coefficient for traction**
Stockholm public transport	approximately 0.15	0.18
U.K.	0.09	0.2
Netherlands	0.07	0.17

2.3 Surface topography

All engineered surfaces are rough to some degree, even when the most advanced surface finishing techniques are used. In most machine elements, surface topography affects friction, wear, and longevity. Moreover, surface topography affects the size of the real contact area [12]. As shown in Fig. 6, surface roughness reduces the nominal contact area to a number of small asperity contact areas ('contacting asperities') that must support the entire normal load. The local pressure in some of these asperities will be greater than that predicted by Herzian theory. According to Marshall et al. [13], maximum pressure between real surfaces is much greater than that predicted by Herzian theory which assumes smooth surfaces. As a result, the high-pressure concentrated area will experience plastic deformation and may work harden, both of which will affect the friction and wear.

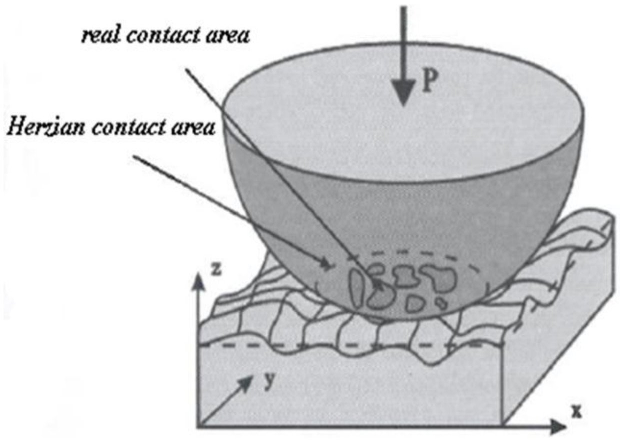

Figure 6. Schematic of contact between rough and smooth surfaces [12].

The surface topography of real wheels and rails is quite variable due to rail grinding and regular use [14][15]. According to Lundmark et al. [14], wheel and rail surfaces can change markedly after just one passing train. Measuring wheel and rail surface topography is difficult. In the field, a quick and repeatable method is to use the MINIPROF system [16]. This system has a small magnetic wheel, approximately 12 mm in diameter, attached to the extremities of two joint extensions. When the magnetic wheel is manually rolled over a surface, the angles of the two extensions are measured and recorded; then the computer can calculate the surface profile. Another way to measure surface topography is to use two-component acrylate plastic to create a negative replica of the original rail surface [4], which is then subjected to 3D surface measurements. However, the accuracy of these techniques are poor [4][17][18]. Some devices [14], such as stylus machines and atomic force microscopes (AFM), can measure the surface topography with high accuracy. Using these devices, both 2D and 3D surface measurements can be made and evaluated in terms of various roughness parameters [19][20]. The two most commonly used 2D parameters are root mean square (RMS) roughness, R_q, and centre-line average (CLA) roughness, R_a, which are defined as follows:

$$R_q = \sqrt{\frac{1}{L}\int_0^L z^2(x)dx} \tag{5}$$

$$R_a = \frac{1}{L}\int_0^L |z(x)|dx \tag{6}$$

where L is the evaluating length and $z(x)$ is the length of the asperity measured from the mean line. However, these measuring devices are heavy, sensitive, and usually time consuming to operate, making them impossible to use in the field. The wheel and rail surface topographies shown in Fig. 7 (the computer illustration with very coarse grids) are of real wheel and rail samples cut in the field in Stockholm [13] and then measured using a stylus instrument. The left image is of an unused or new wheel–rail pair with R_a values of 4.11 and 2.65 μm, respectively. The right image shows two rough surfaces damaged by sand with R_a values of 12.45 and 20.38 μm for the wheel and rail, respectively. Comparing these two surface topographies shows that wheel and rail surfaces differ considerably.

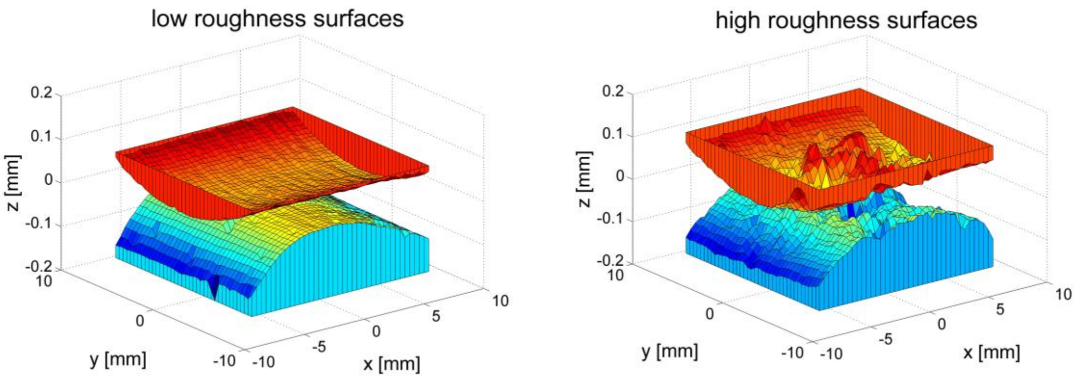

Figure 7. Wheel and rail surfaces of low roughness (left) and high roughness (right).

3 Low adhesion under contaminated conditions

As a rolling–sliding contact, a wheel–rail contact is similar to a rolling ball bearing or gears [1], though these are mostly closed systems with comparatively good lubricating conditions. The wheel–rail contact is an open system, which makes it extremely difficult to transfer knowledge from other well-studied but closed systems. For example, the friction coefficient on the railhead is high on a sunny day but decreases on a rainy day. Even on a sunny day, the friction coefficient can differ depending on the humidity and temperature. In addition, foreign substances, such as sand, dust, leaves, oil or grease, can also be present on the rail. All these factors will influence the friction coefficient, resulting in excessive or insufficient wheel–rail adhesion. Table 2 shows the friction coefficient measured using a hand-push tribometer [1]. The friction coefficient varies depending on the conditions, and is generally reduced by water, oil/grease, and wet leaves. Moreover, temperature and humidity can also change the friction coefficient [21]. Moore [22] presented the typical available friction, i.e., adhesion coefficient, under various conditions as shown in Table 3. Note that sand can increase the adhesion coefficient and moisture can reduce it, compared with outright wet conditions.

Table 2. Friction coefficients measured using a hand-push tribometer [1].

Conditions	Temperature (°C)	Friction coefficient
Sunshine dry rail	19	0.6–0.7
Recent rain	5	0.2–0.3
Substantial grease on rail	8	0.05–0.1
Damp leaf film on rail	8	0.05–0.1

Table 3. Examples of wheel–rail adhesion coefficients [22].

Rail conditions	Adhesion coefficient	Rail conditions	Adhesion coefficient
Dry and clean	0.25–0.3	Moisture	0.09–0.15
Dry with sand	0.25–0.33	Light snow	0.10
Wet and clean	0.18–0.20	Light snow with sand	0.15
Wet with sand	0.22–0.25	Wet leaves	0.07
Greasy	0.15–0.18		

In the context of the railway track, contamination refers to any material that is present on the rail and becomes entrained in the wheel–rail contact. The contamination can be divided into solid contamination, such as sand, dust, leaves, and debris, and liquid contamination, such as water, oil or grease. Of these contaminants, sand is usually used to increase adhesion and remove surface layer contamination, since modern power cars and locomotives require a higher friction coefficient on the railhead [1]. Liquid contaminants and leaves can reduce adhesion, especially when the rolling speed is increasing. Dust or debris could reduce the adhesion by mixing with liquids [23]–[26]. As a result, the dominant problem is too low adhesion in the wheel tread–railhead contact. This thesis focuses mainly on low adhesion in the wheel–rail contact caused by water, oil, and the leaf-formed blackish layer.

Water, which can be in the form of rain, drizzle, or even high humidity, is the most common rail surface contaminant causing low adhesion. Experimental investigation of water as a contaminant that reduces adhesion in the wheel–rail contact started in the UK in the 1970s [23]–[26]. Beagley et al. [23] reported that the adhesion coefficient declined considerably with increased rolling speed under wet conditions. He also pointed out that it was water mixed with wear debris that significantly reduced the adhesion, though the mechanism by which this occurred was still unclear. Oil, which could drip from leaking trains or be deposited at level crossings by vehicle tires or from spilt goods [1], is another typical railhead surface contaminant. Bealgey et al. [23] also investigated the influence of oil on the adhesion coefficient, finding that adhesion did not decrease much with increased speed. Zhang et al. [27] used a full-scale roller rig to simulate the wheel–rail contact under oil-contaminated conditions, finding that adhesion dropped to a very low level, though essentially independently of speed.

Liquid contaminants, such as water and oil, are often used as lubricants in certain industrial applications. Lubricants significantly affect wear and friction and will usually improve the lifetime performance and reliability of a machine. Stribeck [28] studied the effects of lubricants in various lubrication regimes as a function of relative surface velocity (see Fig. 8). In the boundary lubrication regime (BL), the velocity is relatively low. The film build-up is negligible and the load is borne mainly by asperities. The main function of the lubricant is to reduce the adhesion component (i.e., atomic forces) of friction. In the full film lubrication regime (FL), the velocity is high and the two surfaces are fully separated by lubricant; the friction depends mainly on the shear stress in the lubricant. The region between BL and FL is known as the mixed lubrication regime (ML), in which part of the load is borne by asperities and part by lubricant. The friction of ML ranges between those of BL and FL. Elastohydrodynamic lubrication occurs when the surface deformation helps to form a film. The application of the lubrication regime concept to wheel–rail adhesion under water- and oil-lubricated conditions could yield a better understanding of the adhesion-reduction mechanism. Furthermore, since field tests or full-scale tests are usually expensive to run, it is crucial to find a connection between scaled lab tests and the real situation. The Stribeck curve and calculated film thickness parameters could be used to compare scaled tests and the real situation in terms of lubrication regimes, which is very important for selecting parameters and making comparisons in scaled tests.

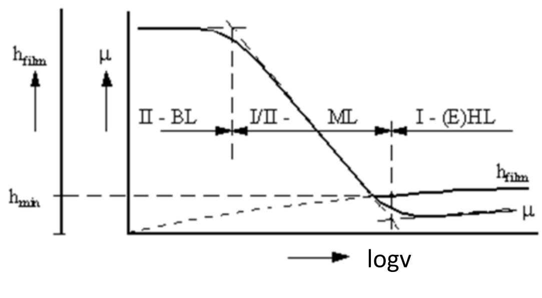

Figure 8. Stribeck curve.

In addition, rail services worldwide are disrupted by fallen leaves. In autumn, leaves fall on the rail lines, forming a blackish layer when they are crushed by passing wheels, resulting in serious adhesion loss. According to Fulford [29], these leaves do not have to fall precisely on the tracks. The turbulence of each passing train stirs up dead leaves that were previously on the track ballast by its slipstream swirling around the vehicle and getting crushed by passing wheels. The crushed leaves eventually form a hard, slippery, blackish layer that strongly adheres to the rail surface and is very difficult and expensive to remove [9][29][31]. This layer gives a friction coefficient of 0.1, or of 0.05 or even less when combined with a small amount of precipitation. Some lab tests [31]–[35] simulating the 'leaves on the line' problem have been conducted, indicating that a chemical reaction occurs on the rail surface resulting in low adhesion. However, the exact mechanism of the layer formation remains unknown, since it is very difficult to run tests that exactly reproduce the real situation. Furthermore, leaves cannot be treated as lubricants, so classical tribology theory cannot be applied. In examining various contaminants, the term 'lubricant' refers to water and oil in the following section.

4 Computer simulation: adhesion modelling under dry and lubricated conditions

A computer simulation is an attempt to model a real-life or hypothetical system on a computer so that it can be studied to see how it works. It is a useful approach for gaining insight into the operation of a system in an economical way. In the wheel–rail contact, computer simulation could be an efficient and repeatable way to study the influence of each parameter based on certain assumptions, since lab or field tests are usually expensive to run and difficult to control.

The complete contact model becomes extremely complicated if all factors are considered, factors such as deformation (e.g., of sleepers, ballast, and even substructures), track characteristics (e.g., irregularity, flexibility, surface roughness, and material properties), and contaminants. Therefore, the wheel–rail contact models developed are more or less based on certain assumptions, such as a rigid wheel and rail, smooth contact surfaces without contamination, and contact as a point contact. Most contact models aim at computing creep force (considering longitudinal, lateral, and spin creep) for vehicle dynamics calculations, which requires short computational time since vehicle running conditions vary greatly. These models [5][36] are based on Hertz's theory of elliptical contact.

However, under conditions of contamination with, for example, water and oil, the contact conditions change. It is well known that in a lubricated contact in which water or oil, for example, is present between the surfaces, a film will form in the interface between the two bodies. The formed film will share part of the normal load and lower the friction coefficient. The formation and effect of the film depend on factors such as surface topography and lubricant properties [37][38]. Therefore, the above-mentioned contact models are not suitable for computing creep force in lubricated contacts, since they assume smooth, uncontaminated surfaces. A new wheel–rail contact model should be developed at the micro level to accommodate contaminated conditions. The new model, as one part of a complete wheel–rail contact model, should investigate adhesion in terms of surface topography and the influence of various contaminants. Some assumptions are made to simplify the problem: the contact is treated as in a static state regardless of dynamic influence (i.e., fixed creep is used as an input to the model) and only longitudinal creep is considered.

The new adhesion model for lubricated conditions needs to include at least three phenomena in order to predict adhesion. The first is normally loaded asperity-to-asperity contact. The second is the pressure build-up in the fluid that interacts with the asperity-to-asperity contact and helps support the normal load. The last is the tangential stress in the rolling and sliding contact due to the tangential loading of the contact. A precursor to this work was conducted by Chen, who presented both 2D [39] and 3D [40] numerical solutions. Both these solutions consider wheel–rail adhesion as an elastohydrodynamic lubrication (EHL) problem, and water viscosity was included in both models. The author applied simple line contact theory in the 2D solution [39], and flow factors developed by

Patir and Cheng [41] in the 3D solution. However, in both solutions, only normally loaded contact and fluid interaction problems were considered. A tangentially loaded contact model was developed based on pure sliding motion. Tomberger et al. [42] proposed a complete contact model that considered all three phenomena mentioned above, and included contact temperature effects as well. According to the effects of the interfacial fluids, the contact range was divided into the dry contact, boundary lubrication, and mixed lubrication regimes. Normally loaded contact and fluid interaction problems were calculated at the micro scale, but viscosity effects were not included in the model. Tangential stress was computed at the macro scale on the basis of Kalker [36]. Popovici [43] developed a wheel–rail friction model considering all three problems at the macro scale. The mixed lubrication problem was divided into two components: the asperity and EHL components. Asperity contact was simplified as the sum of the individual Hertzian contacts of each micro contact. The EHL component was implemented based on film thickness calculations. The contact conditions were treated as a combination of pure rolling and pure sliding contact.

The adhesion models mentioned above are all based on statistical methods, which means that the wheel rail surfaces are described using mathematical methods. According to Björklund [12], there are two ways to model contacts between rough surfaces, i.e., statistical and numerical methods. Statistical methods make use of the stochastic nature of rough surfaces and are not concerned with the exact surface topography. The most-cited statistical model is the Greenwood and Williamson model [44]. On the other hand, numerical methods can be applied to known surface topography, and can model real pressure distribution in the contact patch. Using actual measured 3D surface topographies of wheels and rails as input, the real pressure distribution can be modelled. Numerical methods can also yield information on how real surfaces influence the adhesion coefficient and the fluid film formation.

A numerical model presented in paper **A** for predicting wheel–rail adhesion under dry and lubricated conditions can solve the problem at the micro level. The purpose of that work is to determine how real wheel and rail surfaces influence the adhesion coefficient under dry, water-lubricated, and oil-lubricated conditions. The assumptions are based on elastic contact bodies as infinite half-space with homogeneous and isotropic material. The model presented in paper **A** can be summarized in the framework shown in Fig. 9.

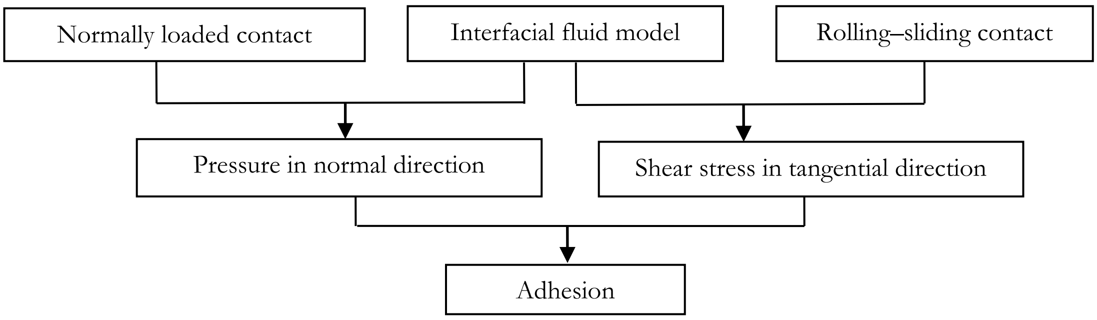

Figure 9. Framework of the numerical model.

- Normal contact model

The surfaces are discretized into a set of elements, each of which corresponds to a uniform pressure. The continuous pressure distribution is then replaced by a discrete set of pressure elements [45]. Given a certain global deformation, which can be regarded as the distance the two contact surfaces would have overlapped without any interaction, each contacting element will deform correspondingly. The real contact area is first estimated as the region the two contact surfaces penetrate without any deformation. The pressure of each element can be found based on the Boussinesq solution. Negative pressure, which indicates that the element is outside the real contact area, should be removed.

- Interfacial fluid model

Since real measured surfaces are used in the model, the gap between the two interacting rough surfaces in which fluid flows can be either convergent or divergent. In the convergent gap, the pressure in the fluid can build up. In the divergent gap, the pressure in the fluid drops, which may generate cavitation when the pressure drops to the ambient level. The solution of the numerical interfacial fluid model differs from those of other models based on statistical methods. The Reynolds equation is then solved in a modified form including cavitation [46]. To balance the load carried by asperities and fluids, an iterative algorithm is used to calculate the actual pressure.

- Rolling–sliding contact model

In modelling a rolling–sliding contact, the contact starts with a stick area and slip occurs when elastic deformation cannot support the relative motion of the two bodies. Based on a particular creep (static situation), the solution starts with the assumption that the whole contact area sticks, and then the shear stress near the trailing edge does not satisfy the boundary condition of limiting friction. These areas are actually slip areas and are removed from the previous stick areas.

As the input to the model, two pairs of measured wheel and rail surfaces (one with high roughness and one with low roughness) along with generated smooth surfaces are used. Simulations are performed under unlubricated and lubricated conditions using the numerical model. Good correlation is found when comparing the results for generated smooth surfaces with widely used approximate nonlinear creep force theory [47][48] under dry conditions. Results also indicate that under dry conditions, the adhesion coefficient peaks at a higher creep with increasing roughness. Under water and oil-lubricated conditions, the maximum adhesion coefficient for low-roughness surfaces is lower than that for high-roughness surfaces, with that for generated smooth surfaces lying between them. Effects of water and oil on the adhesion coefficient are also examined using fluid load capacity. The results indicate that the oil load capacity is greater than the water load capacity. With increased vehicle running speed, the fluid load capacity increases; however, the rate of increase differs between water and oil.

5 Scaled lab test: an MTM study of adhesion under dry and lubricated conditions

In science and technology, a scaled test entails either amplification or reduction of test conditions. A scaled test is of interest when a full-scale test is difficult to perform. Some scaled tests can be conducted in the lab under well-controlled test conditions and are suitable for parameter study.

In research into railway adhesion, some work is done by means of field tests or full-scale tests. Polach [49] studied wheel–rail adhesion under dry and wet conditions using Bombardier and Siemens locomotives in the field at speeds of 30–60 km h^{-1}. Chen et. al [50] and Ohyama [51] used a full-scale twin-disc rolling contact machine to investigate several factors influencing the wheel–rail adhesion coefficient at rolling speeds up to 120 km h^{-1}. Zhang et al. [27] also analyzed wheel–rail adhesion using a full-scale test rig under dry, water-lubricated, and oil-lubricated conditions at speeds up to 280 km h^{-1}. These tests based on locomotives and full-scale test rigs could be run under conditions very close to real ones in terms of axle load, contact geometry, and rolling speed. However, these tests are usually difficult to arrange and/or expensive to run. As a result, many experimental studies [23]–[26] have been performed in the laboratory using scaled test rigs, such as disc–disc, disc-on-cylinder, or disc-on-flat machines. The most common equipment for investigating wheel–rail adhesion under various conditions is the twin-disc machine [9][35]. Because the twin-disc machine can generate rolling–sliding contact, it can simulate the motion of the wheel on the rail. The discs are usually made of real wheel and rail material and the contact pressure is set to be close to the real wheel–rail contact pressure. The maximum rolling speed can range from 1 to 5 m s^{-1} depending on the test set-up. In addition, the pin-on-disc test rig has also been used to simulate the sliding motion in the wheel–rail contact [52]. The above-mentioned scaled test rigs offer the advantages of repeatable, comparatively cheap, and well-controlled testing. However, twin-disc tests are usually conducted based on fixed creep and speed. It is difficult to change the creep and the speed during testing, so full adhesion and Stribeck curves are difficult to obtain. Pin-on-disc testing provides a pure sliding contact that can simulate only the sliding motion of the wheel–rail contact. Recently, Cann [34] used a mini traction machine (MTM) to investigate adhesion in the wheel–rail contact. The MTM is a ball-on-flat test rig that can generate a rolling–sliding contact under a wide range of contact pressures. Moreover, the rolling speed and creep (i.e., the slide–roll ratio in MTM testing) can be changed during testing, so both the adhesion and Stribeck curves can be obtained. It is also possible to specify the temperature of the lubricants in the contact.

A schematic of the MTM is shown in Fig. 10. The test rig consists of a steel ball and a steel disc. The ball is loaded against the face of the disc in what is known as a ball-on-flat contact. The ball and disc can be rotated independently by two motors to generate a rolling–sliding contact. This results in a slide-to-roll ratio (*SRR*), defined as:

$$SRR = \frac{|U_{disc} - U_{ball}|}{(U_{disc} + U_{ball})/2} \tag{7}$$

where U_{disc} and U_{ball} are the velocities of the disc and ball, respectively. The denominator of Eq. 7 is known as the MTM entraining speed.

The ball-on-disc set-up is tested in a closed environment to keep the temperature at the required level. The lateral force exerted on the ball is measured using a force transducer, which further yields the coefficient of friction.

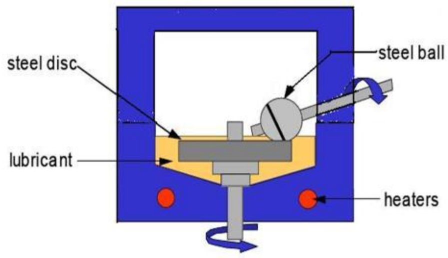

Figure 10. Schematic of the MTM.

The testing can be run in two ways. One way is to keep the entrainment speed constant, increasing (or decreasing) the *SRR* value to obtain an adhesion curve. The other way is to keep the *SRR* value constant, increasing (or decreasing) the entrainment speed to obtain a Stribeck curve. Note that for each entrainment speed, measurements are made with $U_{disc}>U_{ball}$ and $U_{disc}<U_{ball}$, keeping *SRR* constant. The average is taken of the two measurements to remove any offset errors in lateral force measurements. In MTM testing, the *SRR* and entrainment speed can be considered equivalent to creep and rolling speed in railway applications.

Paper **B** presents an experimental study, using an MTM, of adhesion in the wheel–rail contact. This work seeks to determine the influence of several factors, for example, lubricants, rolling speed, and surface roughness, on the adhesion coefficient under dry and lubricated conditions. Testing specimens are discs of two roughnesses (i.e., smooth and rough) and balls; all specimens are made of AISI 52100 steel. The hardness of the disc is approximately 300 HV (close to that of rail material) while that of the ball is 800 HV. Tests are performed to determine both adhesion curves and Stribeck curves. The *SRR* value ranges from 0 to 100% while the entraining speed ranges from 10 to 1500 mm s^{-1}. Tests are performed at two lubricant temperatures (i.e., 5 and 20°C) and contact pressures (i.e., 700 and 900 MPa). The film thickness parameter (lambda) is computed in both scaled tests and real wheel–rail contacts to compare the scale and field tests and determine the relationship between them. The surface topography of the specimens before and after testing is measured and analyzed using the stylus machine. The stylus instrument is a Taylor Hobson Form Talysurf PGI800, which has a stylus tip radius of 2 μm and is traceable to national standards. Atomic force microscopy (AFM) and scanning force microscopy (SFM) are also used for imaging tiny surface scratches found on the disc. AFM is an ultra-high-resolution type of scanning probe microscopy operating at nanometre scale; the instrument consists of a cantilever with a sharp tip (20-nm probe) used to scan the specimen surface. Both 2D and 3D topography are obtained using the above instruments for surface analysis.

In the dry testing, surface roughness did not exert a significant influence on the adhesion coefficient, which ranged from 0.6 to 0.7. In the oil-lubricated testing, surface roughness, contact pressure, and lubricant temperature were found to exert a slight influence on the adhesion coefficient. In the water-lubricated testing, the adhesion coefficient for smooth discs was extremely low at 0.02 compared to 0.2 for rough discs. The value is even lower than those obtained under oil-lubricated conditions. Higher water temperatures (i.e., 5–20°C) were able to increase the adhesion coefficient from 0.15 to 0.2 on rough discs. Surface topography measurements indicated only small scratches on the water-lubricated smooth discs. The number of scratches is fewer and their depth less than those on oil-lubricated discs. Rough discs tested under water-lubricated conditions display a clear wear track. Comparison of the experiments using the MTM with those using the real wheel–rail contact is presented in terms of lubrication regime based on lambda value calculations.

6 Field test: a study of leaf contamination on the railhead

A field test is a test conducted under actual operating conditions instead of under controlled conditions in a laboratory. Compared with a lab test, a field test can reflect the real situation but usually under very complex conditions.

With regard to adhesion in the wheel–rail contact, the low adhesion caused by leaf contamination is more complicated than wheel–rail adhesion under lubricated conditions. In the cases of water and oil, we already have some data on the lubricants and it is also possible to measure their unknown properties. However, we know little about leaves and the associated low adhesion problem, though low adhesion caused by leaf contamination is severe and widespread. Fulford [8] reports that the leaf-formed blackish layer gives a very low friction coefficient, which becomes even lower with the presence of a small amount of precipitation. These blackish layers are extremely difficult to remove [31]. According to the Swedish national railroad administration, the cost associated with 'leaves on the line' in Sweden was estimated to be SEK 100 million annually as of 1996 [29], and the annual cost was reportedly GBP 50 million in the United Kingdom as of 2001 [30]. In the Netherlands, extremely low adhesion one day in autumn 2002 increased wheel defects by 20%, forcing the rail operator to halt service on most of the network that day [9]. In this decade, some tests have been conducted to simulate the 'leaves on the line' problem. Poole [53] used a full-scale test rig to produce leaf film in the laboratory, in order to compare the results with those from the field. Olofsson and Sundvall [31] carried out pioneering work to simulate leaf contamination using a pin-on-disc machine in the laboratory, while Olofsson himself presented a multi-layer model [32] of the contaminated rail surface. In devising this model, he measured the friction coefficient on the leaf-contaminated surface and other related factors [32]. The chemical composition of these contaminated surfaces was analyzed using glow discharge optical emission spectrometry (GD-OES). In addition, Gallardo-Hernandez and Lewis [35] and Arias-Cuevas [33] simulated leaf contamination using a twin-disc machine. Cann [34] used an MTM to study the 'leaves on the line' problem, and found that the pectin and cellulose in the film resulted in the low friction coefficient. The blackish layer was formed by chemical reactions between leaves and the bulk material. However, all these results were obtained from lab testing. Since we still do not understand the actual mechanism by which leaves cause low adhesion, it is necessary to investigate the real situation, as it includes all potential factors. Therefore, field testing is best suited for studying leaf contamination on the railhead and can provide complementary results for comparison to lab testing results.

Paper **C** presents a field test study of leaf contamination on the railhead surface. The work seeks to determine the characteristics of the leaf-contaminated layer and their connection to the low friction coefficient. The test track is part of the Stockholm Underground track system operated and maintained by Stockholm Public Transport AB (SL). The test track, a parallel straight section near the Brommaplan underground station, has a long history of adhesion problems. Over the course of one year, the friction coefficients of rail sections were measured in five periods (i.e., June 2008, September 2008, October 2008, November 2008, and March 2009) using a hand-push tribometer; rail samples were cut in each period for surface analysis. The surface analysis techniques used in this study are described below.

- Electron spectroscopy for chemical analysis (ESCA)

ESCA, also known as X-ray photoelectron spectroscopy (XPS), is a quantitative spectroscopic technique that measures the elemental composition and chemical state of elements in the analysed material. The spectra are obtained by irradiating a material with a beam of X-rays while simultaneously measuring the kinetic energy and number of electrons that escape from the top 1 to 10 nm of the material. The raw ESCA spectrum results comprise a plot of detected electrons versus their binding energy. Each element produces characteristic peaks at characteristic binding energies, which can be directly identified as each element present in the surface of a material. The number of detected electrons in each characteristic peak is directly related to the amount of the element in the irradiated area. Some examples of ESCA spectra are shown and discussed in Olefjord et al. [54].

- Glow discharge optical emission spectrometry (GD-OES)

GD-OES is an analytical technique widely used for the elemental and depth profiling analysis of materials. The depths amenable to such analysis range from a few nanometres to approximately 100 μm. In GD-OES, the test specimen forms the cathode in a glow discharge lamp. The discharge support gas is usually argon. A low-power argon plasma is initiated by the applied high potential between two electrodes (known as the d.c. glow discharge source) [55]. The applied high potential causes the discharge gas to break down electrically to form electrons and positively charged ions. The positive ions are attracted towards the sample surface by the electric fields within the plasma, which may reach substantial kinetic energies. When an ion strikes the sample surface with sufficient energy, the transfer of momentum into the atomic lattice structure of the surface may cause the release of surface material into gas phase, in a process known as 'sputtering'. The sputtered material then undergoes a larger number of collisional processes, such as electronic excitation, that make the sputtered material exist in the glow charge as excited state species. Photons, which are emitted by the excited state species in the plasma, can be measured and analyzed based on elements' characteristics. The emission intensities as a function of sputtering time yield elemental depth profiles. To quantify the recorded depth profiles involving sputtering through layers of highly varying composition, special calculation algorithms for quantifying sputtered depth and elemental mass fractions are used. The method is capable of detecting all chemical elements. More details of GD-OES and a comparison with EXCA are discussed by Dizdar [56] and Bengtson [57].

Hand-push tribometer measurements indicate that the friction coefficient in the contaminated period is only 0.15, which is quite low compared with the results from other periods. Note that the maximum friction coefficient recorded in these tests is 0.7 for dry uncontaminated rail. Surface analysis results indicate that high amounts of calcium, carbon, and nitrogen and a reduced amount of iron are found only in the blackish layer. The distributions of other elements, from the outermost surface and a depth of several microns below the surface, in the blackish layer also differ from other samples. Samples taken on other occasions and those taken on the same occasion but without the blackish layer do not display the same characteristics. The thickness of the friction-reducing oxide layer, D_0 (see Fig. 11) [58][59], is calculated based on the depth profiles of the iron and oxygen contents. Nano-indentation tests indicate that the blackish layer is softer than the uncontaminated layers.

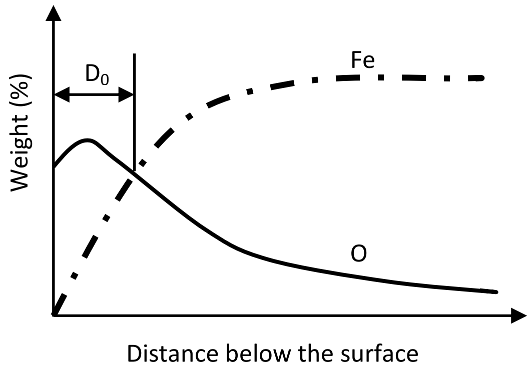

Figure 11. Schematic depth profile. The thickness of the friction-reducing oxide layer is D_0.

7 Concluding remarks

The concluding remarks take the form of answers to the research questions. The research questions can be divided into two groups, one related to water- and oil-lubricated contacts and the other to leaf contamination. The former is discussed in papers **A** and **B**, while the latter is discussed in paper **C**.

- *How does surface topography affect wheel–rail adhesion under water-lubricated conditions?*

This question was addressed using both numerical simulation and lab testing. The numerical study found that the adhesion coefficient for low-roughness surfaces was lower than that for high-roughness surfaces, with that for generated smooth surfaces lying between them, though the difference among the three was fairly small. With increased speed, the reduction of the adhesion coefficient was also small. Water can reduce the limiting friction from 0.52 (dry) to 0.17, as measured on the rail section. According to fluid load capacity results, only a very small part of the load is borne by water, most of the load being carried by asperities. This indicates that a water-lubricated contact is boundary lubricated because of the low viscosity of water; this finding is in line with the minimum film thickness calculated by Hamrock [60]. However, experimental results indicate a significant difference between the adhesion coefficients for smooth and rough discs. The measured and numerically simulated adhesion coefficients are similar for rough discs, but the adhesion coefficient for smooth surfaces is extremely low. Full-scale lab testing and field testing also indicate that wheel–rail adhesion under wet conditions decreases significantly with increasing speed [51], a phenomenon not attributable to the hydrodynamic effect of fluids. As a result, chemical reaction or the particular water–contaminant mixture may have an essential impact on wheel–rail adhesion. Beagley and Pritchard [25] found that the presence of water in a stainless steel contact could reduce the friction coefficient only from 0.7 to 0.57, indicating that the effect of pure water was very limited. Beagley [26] also suggested that the presence of a small amount of oil in water substantially reduced the friction, the extent of the reduction depending on the amount of oil present. Furthermore, water mixed with wear debris could be reduce adhesion greatly because of the high viscosity of the mixture [26]. In boundary lubrication, chemical reactions are also important; for example, the presence of a thin oxide layer on the surface can give very low friction [56][61][62]. However, neither the water–contaminant mixture nor the chemical reaction could be simulated by the present model. The influence of surface topography under water-lubricated conditions was investigated by Chen et al. [50] using both a full-scale and a scaled test rig; the authors used three kinds of abrasive paper, i.e., #80, #320, and #800, to generate three levels of surface roughness with R_q values of 2.01, 0.78, and 0.53 μm, respectively. Results indicated that increasing roughness would increase the adhesion coefficient, in line with the results presented here.

- *How does surface topography affect wheel–rail adhesion under oil-lubricated conditions?*

This question was addressed using both numerical modelling and lab testing. The results of the numerical model correlated with those of the lab testing under oil-lubricated conditions. The adhesion coefficient for low-roughness surfaces is lower than that for high-roughness surfaces, because rough surfaces negatively affect film formation, reducing the fluid load capacity. However, the adhesion coefficient for the generated smooth surface is between those for the two measured surfaces. This can be explained by the 'pocket' effect found by Zhu and Hu [37]. Surface roughness is helpful in the boundary lubrication regime, as it can generate 'pockets' that retain lubricant in the contact. As a result, the fluid load capacity of low-roughness surfaces is higher than that of perfectly smooth surfaces, resulting in a lower adhesion coefficient for low-roughness surfaces. When the surface topography is very rough, for example, in the case of the high-roughness surfaces shown in Fig. 7, the 'pocket' effect disappears because the film pressure in the 'pocket' areas decreases. The conclusion that the adhesion coefficient increases with increasing surface roughness is true only for relatively rough surfaces, while the opposite is the case for relatively smooth surfaces. The lubrication regimes prevalent under oil-lubricated conditions are as follows: on extremely smooth surfaces, the effects of elastohydrodynamic lubrication are marked particularly with increasing speed; on medium-smooth surfaces, mixed lubrication prevails; while on rough surfaces, boundary lubrication dominants. This conclusion agrees well with lambda calculations for real wheel–rail contacts, indicating that the lubrication regime in oil-lubricated wheel–rail contacts varies from boundary to elastohydrodynamic depending on the speed and surface roughness. An early experimental investigation [51] classified wheel–rail adhesion under oil-lubricated conditions as boundary lubrication; this might not always be correct, since the lubrication regime depends on the surface roughness and speed. Beagley et al. [23] found that variation in wheel–rail adhesion was also associated with changes in the quantity of oil on the surface. Unfortunately, it is very difficult to change the amount of lubricant when using an MTM, since the contact is submerged in the lubricant. In numerical simulation, it is also very tricky to specify the viscous effect of the lubricant according to the amount.

- *Do other factors affect wheel–rail adhesion?*

Yes, many other factors do affect adhesion in the wheel–rail contact, as follows:

1) Speed and creep. Note that the speed investigated in paper **A** is vehicle running speed while in paper **B** it is rolling speed; creep in paper **B** is called *SRR*. The relationships between these parameters are explained in the two papers. In the low creep range, the adhesion coefficient increases with increased creep because the slip region increases in extent. When creep reaches a certain value, gross slip appears, at which point speed is the governing factor. With increased speed, the adhesion coefficient decreases, since increased speed will increase the fluid load capacity.

2) Lubricant temperature. This is discussed in paper **B**. Under water-lubricated conditions, increasing the water temperature from 5 to 20°C can increase the adhesion coefficient for rough discs. However, similar behaviour is not apparent for smooth discs or under oil-lubricated conditions.

3) Contact pressure. This is discussed in paper **B**. Higher contact pressure will increase the adhesion coefficient under water-lubricated conditions, but only for rough surfaces. Under oil-lubricated conditions, the influence of oil temperature is very slight.

- *What is the chemical composition of the leaf-contaminated blackish layer, and how does it differ from those of uncontaminated layers?*

The surface analysis indicates the chemical composition of the leaf-contaminated blackish layer differs greatly from that of the uncontaminated layers, when sampled both on the same and different occasions. Significantly large amounts of carbon, calcium, oxygen, and nitrogen and a reduced amount of iron were found in the blackish layer. In addition, the blackish layer also differs distinctly from that of other samples in the contents of other elements. These results indicate that the leaves chemically reacted with the bulk material to form the blackish layer. Hardness testing also indicates that the blackish layer is softer than the uncontaminated layers.

- *Why does the presence of a leaf-contaminated blackish layer on the railhead surface give a low friction coefficient?*

The thickness of the friction-reducing oxide layer is very closely correlated with the friction coefficient; however, the blackish layer is the thickest layer and gives the lowest friction coefficient. It is not the leaves themselves that cause the low friction coefficient but the blackish layer which is formed by leaves chemically reacted with the bulk material. The depth profiles of the iron and oxygen contents are useful to predict the friction coefficient. However, the possibility that other elements may also affect the friction coefficient merits further examination.

Based on the present results, the following further research would be productive:

- *The numerical model could be further improved by including the effects of contact temperature, plastic deformation, and the presence of an easily sheared surface layer.*
- *The experimental work could be further improved by studying the effects of surface texture and the oxide layer in combination with water or other contaminants.*

8 References

[1] Lewis R., Olofsson U.: *Wheel–rail interface handbook*, Woodhead Publishing Limited, Cambridge, UKs, 2009, pp. 24, 284, 437, 510, 514.

[2] Esveld C.: *Modern railway track*, 2nd edition, ISBN 90-800324-3-3, 2001

[3] Lewis R., Olofsson U.: Mapping rail wear regimes and transitions, *Wear* 257 (2004), pp. 721–729

[4] Olofsson U., Telliskivi T.: Plastic deformation and friction of two rail steels: a full-scale test and a laboratory study, *Wear* 254(2003), pp. 80–93

[5] Carter F.W.: On the action of a locomotive driving wheel, *Proceedings of Royal Society of London* A112 1912, pp. 151–157.

[6] Kalker J.J.: Wheel–rail rolling contact theory, *Wear* 144 (1991), pp. 243–261.

[7] ASM handbook, Vol.18: friction, lubrication, and wear technology. *ASM international* 1992

[8] Fulford C.R.: *Review of low adhesion research,* published by Rail Safety and Standards Board (May 2004)

[9] Arias-Cuevas O.: *Low adhesion in the wheel–rail contact*, Doctoral thesis, TUD, Delft, 2010

[10] Jacobsson M.: *Teknikforum Halt Spår*, Technical report (in Swedish), Stockholm Local Traffic, Mar. 2011.

[11] Baek K., Kyogoku K., Nakahara T.: An experimental study of transient traction characteristic between rail and wheel under low slip and low speed conditions, *Wear* 265(2008), pp. 1417–1424.

[12] Björklund S.: *Elastic contacts between rough surfaces*, Doctoral thesis, KTH, Stockholm, 1995

[13] Marshall M.B., Lewis R., Dwyer-Joyce R.S., Olofson U., Björklund S.: Experimental characterization of wheel–rail contact patch evolution, *J. Tribol.* 128/3 (2006), pp. 493–504.

[14] Lundmark J., Höglund E., Prakash B.: Running-in behaviour of rail and wheel contacting surfaces, AITC-AIT 2006, *International Conference on Tribology*, Parma, Italy, 20–22 Sept. 2006.

[15] Chen H., Ishida M.: influence of rail surface roughness formed by rail grinding on rolling contact fatigue, *QR of RTRI*, Vol.47, No.4, 2006

[16] Esveld C.: MINIPROF: wheel and rail measuring equipment, Esveld Consulting Services BV, The Netherlands

[17] Sundh J.: *On the wear transitions in the wheel–rail contact*, Doctoral thesis, KTH, Stockholm, 2009

[18] Ohlsson O., Rosen B.: On replication and 3D stylus profilometry techniques for measurement of plateau-honed cylinder liner surfaces, in: R. J. Hocken (Ed.), *Proceedings of the ASPE 1993 Annual Meetings*, Seattle, Washington, USA, 7–12 November 1993

[19] Thomas T.R.: *Roughness surfaces*, 2nd edition, Imperial college press, 1999

[20] Whitehouse D.J.: *Handbook of surface and nanometrology*, ISBN 0 7503 0583 5, Institute of physics publishing, 2003

[21] Lewis R., Lewis S., Zhu Y., Abbasi S., Olofsson U.: The modification of a slip resistance meter for measurement of railhead adhesion*, Proceedings of International Heavy Haul Association Conference 2011*, Calgary, Canada.

[22] Moore D.F. *Principles and Applications of Tribology*, Elsevier, Amsterdam (1998)

[23] Beagley T.M., Mcewen I.J., Pritchard C.: Wheel/rail adhesion: boundary lubrication by oily fluids, *Wear* 31 (1975) 77–88.

[24] Beagley T.M., Mcewen I.J., Pritchard C.: Wheel/rail adhesion: the influence of railhead debris, *Wear* 33 (1975) 141–152.

[25] Beagley T.M., Pritchard C.: Wheel/rail adhesion: the overriding influence of water, *Wear* 35 (1975) 299–313.

[26] Beagley T.M., The rheological properties of solid rail contaminants and their effect on wheel/rail adhesion, *Proc. Instn. Mech. Engrs.* 190 (39) (1976) 419–428.

[27] Zhang W., Chen J., Wu X., Jin X.: Wheel/rail adhesion and analysis by using full scale roller rig, *Wear* 253 (2002) 82–88.

[28] Stribeck R., Die wesentlichen eigenshaften der Gleit-und rollenlager, Zeitschrift des vereins deutcher ingenieure, 46 pp. 1341–1348, 1432–1438, and 1463–1470

[29] Forslöv L., wheel slip due to leaf contamination, *Swedish National Rail Administration TM* 1996 03 19, Borlänge, Sweden, 1996

[30] Managing low adhesion, Report published by the Adhesion Working Group, UK, (September 2001)

[31] Olofsson U., Sundvall K.: Influence of leaf, humidity and applied lubrication on friction in the wheel–rail contact: pin-on-disc experiments*, Proc. Instn Mech. Engrs Vol. 218 Part F: J. Rail and Rapid Transit*, 2004

[32] Olofsson U.: A multi-layer model of low adhesion between railway wheel and rail, *Proc. Instn Mech. Engrs Vol. 221 Part F: J. Rail and Rapid Transit,* 2007

[33] Arias-Cuevas O.: Investigation some sanding parameters to improve the adhesion in leaf contaminated wheel–rail contacts. *Proc. Instn Mech. Engrs Vol. 224 Part F: J. Rail and Rapid Transit,* 2010, pp. 139–157

[34] Cann P.M.: The 'leaves on the line' problem: a study of leaf residue film formation and lubricity under laboratory test conditions*, Tribology letters,* Vol. 24, No. 2, 2006, pp. 151–158

[35] Gallardo-Hernandez E.A., Lewis R.: Twin disc assessment of wheel/rail adhesion, *Wear* 265 (2008) 1309–1316.

[36] Kalker J. J., A fast algorithm for the simplified theory of rolling contact*, Vehicle System Dynamics* 11 1982, pp. 1–13

[37] Zhu D., Hu Y.: A computer program package for the prediction of EHL and mixed lubrication characteristics, friction, subsurface stresses and flash temperatures based on measured 3-D surface roughness, *Tribology Trans.* Vol. 44(2001), 3, pp. 383–390

[38] Bergseth E.: *Influence of surface topography and lubricant design in gear contacts*, Licentiate thesis, Royal Institute of Technology, Department of machine Design, Stockholm, Sweden, 2009

[39] Chen H., Ban T., Ishida M., Nakahara T.: Adhesion between rail/wheel under water lubricated contact, *Wear* 253(2002), pp. 75–81.

[40] Chen H., Ishida M., Nakahara T.: Analysis of adhesion under wet conditions for three dimensional contact considering surface roughness, *Wear* 258 (2005), pp. 1209–1216.

[41] Patir N., Chen H.S., Effects of surface roughness orientation on the central film thickness in EHD contact, *Proceedings of the 5th Leeds–Lyon Symposium on Tribology,* 1978, pp. 15–21

[42] Tomberger C., Dietmaier P., Sextro W., Six K.: Friction in wheel–rail contact: a model comprising interfacial fluids, surface roughness and temperature, *8th International Conference on Contact Mechanics and Wear of Rail/Wheel System (CM2009)*, Firenze, Italy, 15–18 September 2009, pp. 121–132.

[43] Popovici R.I.: *Friction in wheel–rail contact*, Doctoral thesis, University of Twente, Department of Engineering Technology, Enschede, Netherlands (2010).

[44] Greenwood J.A., Williamson J.B.P.: Contact of nominally flat surfaces, *Proc. R. Soc. Lond.* A 6, 295/1442 (1966), pp. 300–319.

[45] Björklund S., Andersson S.: A numerical method for real elastic contacts subjected to normal and tangential loading, *Wear* 179 (1994), pp. 117–122.

[46] Ausas R.F., Jai M., Buscaglia G.G.: A mass-conserving algorithm for dynamical lubrication problems with cavitation*, J. Tribol.* 131/3 (2009), pp. 1–7.

[47] R.C. White, D.A. Limbert, J.K. Hederick, N.K. Cooperrider: *Guideway–Suspension Tradeoffs in Rail Vehicle Systems*, report DOT-OS-50107, Washington DC (1978).

[48] Z.Y. Shen, L. Hedrick, and J.A. Elkins: A comparison of alternative creep-force models for rail vehicle dynamic analysis, *Proc. of 8th IAVSD Symposium on Dynamics of Vehicles on Roads and on Tracks*, Boston, MA (1983), pp. 591–605.

[49] Polach O.: Creep forces in simulations of traction vehicles running on adhesion limit, *Wear* 258 (2005), 992–1000.

[50] Chen H., Ban T., Ishida M., Nakahara T.: Experimental investigation of influential factors on adhesion between wheel and rail under wet condition, *Wear* 265 (2008) 1504–1511.

[51] Ohyama T.: Tribological studies on adhesion phenomena between wheel and rail at high speeds, *Wear* 144 (1991) 263–275.

[52] Sundh J., Olofsson U., Sundvall K.: Seizure and wear rate testing of wheel–rail contacts under unlubricated conditions using pin-on-disc methodology, *Wear* 265 (2008) 1425–1430.

[53] Poole W.: Characteristics of railhead leaf contamination, summary report published by Rail Safety and Standards Board (May 2007)

[54] Olefjord I., Brox B. and Jelvestam J.: Surface composition of stainless steels during anodic dissolution and passivation studied by ESCA, *J. Electrochem. Soc.* Vol 132(1985) 2854–2861.

[55] Winchester M.R., Payling R.: Radio-frequency glow discharge spectrometry: A critical review, *Spectrochimica Acta Part B* 59 (2004) pp. 607–666

[56] Dizdar S.: *Formation and failure of chemireacted boundary layers in lubricated steel contacts*, Doctoral thesis, KTH, Stockholm, 1999

[57] Bengtson A.: Summary of ISO/TC 201 Standard: III ISO 14707:2000 – Surface chemical analysis – Glow discharge spectrometry – Glow discharge optical emission spectrometry – Introduction for use Surf. *Interface Anal.* 2002; 33: pp. 363–364

[58] Zhao Y.W., Liu J.J., Zheng L.Q.: The oxide film and oxide coating on steels under boundary lubrication. *Proceedings of 16th Leeds–Lyon Symposium on Tribology* (1989), pp. 305–311.

[59] Zhao Y.W., Liu J.J.: The nature of the friction transition as a function of load and speed for the steel/steel system, *ASME/STLE Tribol. Trans.* 33(1990), pp. 648–652.

[60] Hamrock B.J.: *Fundamental of fluid film lubrication*, NASA, 1991

[61] Baek K-S., Kyogoku K., Nakahara T.: An experimental investigation of transient traction characteristics in rolling–sliding wheel/rail contacts under dry–wet conditions, *Wear* 263 (2007), pp. 169–179

[62] Nakahara T., Baek K-S., Chen H., Ishida M.: Relationship between surface oxide layer and transient traction characteristics for two steel rollers under unlubricated and water lubricated conditions, *Wear* 271 (2011), pp. 25–31